



U.S. DEPARTMENT OF  
**ENERGY** | Office of  
Science

DOE/SC-ARM-TR-020

## **Ceilometer Instrument Handbook**

VR Morris

April 2016



## **DISCLAIMER**

This report was prepared as an account of work sponsored by the U.S. Government. Neither the United States nor any agency thereof, nor any of their employees, makes any warranty, express or implied, or assumes any legal liability or responsibility for the accuracy, completeness, or usefulness of any information, apparatus, product, or process disclosed, or represents that its use would not infringe privately owned rights. Reference herein to any specific commercial product, process, or service by trade name, trademark, manufacturer, or otherwise, does not necessarily constitute or imply its endorsement, recommendation, or favoring by the U.S. Government or any agency thereof. The views and opinions of authors expressed herein do not necessarily state or reflect those of the U.S. Government or any agency thereof.

# **Ceilometer Instrument Handbook**

VR Morris, Pacific Northwest National Laboratory

April 2016

Work supported by the U.S. Department of Energy,  
Office of Science, Office of Biological and Environmental Research

## Acronyms and Abbreviations

AGL	above ground level
AMF	ARM Mobil Facility
ARM	Atmospheric Radiation Measurement Climate Research Facility
CEIL	Ceilometer
DOE	U.S. Department of Energy
DQPR	Data Quality Problem Report
DQR	Data Quality Report
ENA	Eastern North Atlantic, an ARM site
Km	kilometer
lidar	light detection and ranging
m	meter
mm	millimeter
MOR	Meteorological Optical Range
MPL	Micro Pulse Lidar
mrاد	milliradian
nm	nanometer
ns	nanosecond
NSA	North Slope of Alaska, an ARM site
QME	Quality Measurement Experiment
SGP	Southern Great Plains, an ARM megasite
VAC	volts, alternating current
VAP	Value-Added Product

## Contents

Acronyms and Abbreviations .....	iii
1.0 General Overview .....	1
2.0 Contacts .....	1
2.1 Mentor .....	1
3.0 Deployment Locations and History .....	1
4.0 Near-Real-Time Data Plots .....	4
5.0 Data Description and Examples .....	4
5.1 Data File Contents .....	5
5.1.1 Primary Variables and Expected Uncertainty .....	6
5.1.2 Secondary/Underlying Variables .....	7
5.1.3 Diagnostic Variables .....	7
5.1.4 Data Quality Flags .....	8
5.1.5 Dimension Variables .....	9
5.2 User Notes and Known Problems .....	10
5.3 Frequently Asked Questions .....	10
6.0 Data Quality .....	11
6.1 Data Quality Health and Status .....	11
6.2 Data Reviews by Instrument Mentor .....	11
6.3 Data Assessments by Site Scientist / Data Quality Office .....	12
6.4 Value-Added Procedures and Quality Measurement Experiments .....	12
7.0 Instrument Details .....	13
7.1 Detailed Description .....	13
7.1.1 List of Components .....	13
7.1.2 System Configuration and Measurement Methods .....	13
7.1.3 Specifications .....	15
7.2 Theory of Operation .....	15
7.3 Calibration .....	17
7.3.1 Theory .....	17
7.3.2 Procedures .....	18
7.3.3 History .....	18
7.4 Operation and Maintenance .....	18
7.4.1 User Manual .....	18
7.4.2 Routine and Corrective Maintenance Documentation .....	18
7.4.3 Software Documentation .....	19
7.5 Glossary .....	19

7.6 Acronyms ..... 19  
7.7 Citable References..... 19

## Figures

1. CL-View cloud intensity graph (0 – 25500 ft AGL). ..... 5

## Tables

1. History of deployment locations..... 2  
2. Primary variables. .... 6  
3. Secondary variables. .... 7  
4. Diagnostic variables..... 7  
5. Data quality flags. .... 8  
6. Data quality thresholds. .... 8  
7. Time quality flags. .... 9  
8. Dimension variables. .... 9  
9. Vaisala CL31 main parts..... 13  
10. Vaisala CL31 configuration settings..... 14  
11. Specifications of CL31 ceilometer, as operated at ARM sites. .... 15

## 1.0 General Overview

The Vaisala Laser Ceilometer (CEIL) is a self-contained, ground-based, active, remote-sensing device designed to measure cloud-base height, vertical visibility, and potential backscatter signals by aerosols. It detects up to three cloud layers simultaneously. Model CL31 has a maximum vertical range of 7700 meters (m). The laser ceilometer transmits near-infrared pulses of light, and the receiver detects the light scattered back by clouds and precipitation.

## 2.0 Contacts

### 2.1 Mentor

Victor Morris  
Pacific Northwest National Laboratory  
P.O. Box 999, MS K9-24  
Richland, WA 99352  
Phone: 09-372-6144  
E-mail: [vic.morris@arm.gov](mailto:vic.morris@arm.gov)

## 3.0 Deployment Locations and History

The U.S. Department of Energy (DOE)'s Atmospheric Radiation Measurement (ARM) Climate Research Facility currently operates a total of six laser ceilometers at its fixed sites (in Oklahoma, Alaska, and the Azores) and its mobile facilities (AMF). Initially, a [Belfort 7013C Laser Ceilometer](#) was deployed at the ARM Climate Research Facility Southern Great Plains (SGP) site in 1994 and was replaced with a Vaisala CT25K Ceilometer in 2000. Meanwhile, additional CEILs were gradually deployed at all other ARM sites, including the now-decommissioned Tropical Western Pacific sites, between 1996 and 2004. Through the American Recovery and Reinvestment Act, six of the ceilometers were replaced in 2010 with the Vaisala CL31, which provides greater spatial and temporal resolution, improved algorithms for cloud amount and mixing layer height, and better detection of aerosol layers.

**Table 1.** History of deployment locations.

Current status = operational, spare, failure, or decommissioned

Model number	Serial number	Site	Start date	End date
CL31	J3110011	AWR/S1	11/19/2015	present
CL31	H2310002	OLI/M1	08/29/2013	present
CL31	H2320001	ENA/C1	09/29/2013	present
CL31	F1040006	SBS/M1	09/24/2010	05/01/2011
CL31	F1040006	GAN/M1	10/01/2011	04/03/2012
CL31	F1040006	MAG/M1	09/26/2012	09/26/2013
CL31	F1040006	TMP/M1	01/16/2014	09/15/2014
CL31	F1040006	ACX/M1	12/17/2014	02/18/2015
CL31	F1040006	AWR/M1	11/19/2015	present
CL31	F1040005	GRW/M1	07/15/2010	01/21/2011
CL31	F1040005	PGH/M1	05/31/2011	04/01/2012
CL31	F1040005	PVC/M1	07/04/2012	06/30/2013
CL31	F1040005	MAO/M1	12/21/2013	12/01/2015
CL31	F1040004	TWP/C3	08/16/2010	12/31/2014
CL31	F1040003	TWP/C1	08/26/2010	06/30/2014
CL31	F1040002	NSA/C1	06/16/2010	present
CL31	F1040001	SGP/C1	04/16/2010	present
CT25K	Z11201	PYE/M1	02/01/2005	09/15/2005
CT25K	Z11201	NIM/M1	11/23/2005	01/08/2007
CT25K	Z11201	FKB/M1	03/12/2007	01/18/2008
CT25K	Z11201	HFE/M1	05/01/2008	12/30/2008
CT25K	Z11201	GRW/M1	05/16/2009	07/15/2010
CT25K	Z11201	ALTOS	10/01/2010	04/01/2011
CT25K	Z11201	MAO/S1	12/21/2013	12/01/2015
CT25K	V45106	TWP/C3	02/27/2002	12/09/2002
CT25K	V45106	NIES	02/08/2003	07/01/2003
CT25K	V45106	TWP/C2	04/17/2007	11/26/2012
CT25K	V45105	NIES	12/22/2001	02/08/2003
CT25K	V45105	Vaisala	03/25/2003	10/20/2003
CT25K	V45105	TWP/C1	12/06/2003	08/26/2010
CT25K	V36301	HFE/S1	07/29/2008	12/15/2008
CT25K	U06301	SGP/B6	01/05/2001	08/31/2007
CT25K	U06301	TWP/C2	11/26/2012	09/15/2013

Model number	Serial number	Site	Start date	End date
CT25K	T24501	TWP/C1	01/13/2000	06/24/2001
CT25K	T24501	Vaisala	07/20/2001	12/03/2001
CT25K	T24501	TWP/C1	01/18/2002	12/06/2003
CT25K	T24501	TWP/C2	04/01/2005	02/04/2007
CT25K	T24501	Vaisala	04/26/2007	07/30/2007
CT25K	T24501	SGP/B6	08/31/2007	01/13/2010
CT25K	S17102	NSA/C1	12/12/1997	12/03/2009
CT25K	R0850006	SGP/B4	09/20/1999	07/23/2002
CT25K	R0850006	TWP/C3	12/09/2002	12/12/2005
CT25K	R0850006	Vaisala	03/06/2006	04/27/2006
CT25K	R0850006	TWP/C3	05/18/2006	12/20/2006
CT25K	R0850006	TWP/C3	01/12/2007	01/16/2007
CT25K	R0850006	TWP/C3	01/19/2007	07/11/2007
CT25K	R0850006	Vaisala	09/10/2007	10/18/2007
CT25K	R0850006	SGP/B5	10/23/2007	11/07/2007
CT25K	R0850006	SGP/B5	02/27/2008	01/17/2009
CT25K	R0850006	NSA/C1	12/03/2009	06/15/2010
CT25K	R0850004	SGP/B5	09/21/1999	04/26/2001
CT25K	R0850004	SGP/B4	07/23/2002	01/07/2003
CT25K	R0850004	SGP/B4	05/10/2004	02/17/2010
CT25K	R0850004	FACETS	04/01/2011	11/30/2014
CT25K	R0850003	SGP/B6	09/21/1999	08/24/2000
CT25K	R0850003	SGP/B1	11/24/2000	10/20/2009
CT25K	R0850003	ICECAPS	04/01/2010	present
CT25K	R0850002	SGP/B1	09/20/1999	08/29/2000
CT25K	R0850002	SGP/B5	04/26/2001	07/14/2005
CT25K	R0850002	SGP/C1	04/19/2006	04/16/2010
CT25K	R0850002	FACETS	04/01/2011	11/30/2014
CT25K	R0850002	MCQ/C1		
CT25K	R0450013	NSA/C2	08/22/1999	01/17/2011
CT25K	P2710016	SGP/C1	05/22/2000	12/06/2004
CT25K	P2710016	SGP/B5	07/14/2005	10/23/2007
CT25K	P2710016	SGP/B5	11/08/2007	02/27/2008
CT25K	P2710016	GRW/M1	04/20/2009	05/16/2009
CT25K	P2710016	Vaisala	07/30/2009	01/27/2010

Model number	Serial number	Site	Start date	End date
CT25K	P2710015	TWP/C2	12/22/1995	09/23/2002
CT25K	P2710015	Vaisala	10/28/2002	01/03/2003
CT25K	P2710015	SGP/B4	01/07/2003	05/10/2004
CT25K	P2710015	SGP/C1	12/06/2004	04/19/2006
CT25K	P2710015	TWP/C3	01/16/2007	01/19/2007
CT25K	P2710015	TWP/C2	02/05/2007	04/17/2007
CT25K	P2710015	Vaisala	05/21/2007	07/30/2007
CT25K	P2710015	TWP/I10	08/15/2011	01/18/2013
CT25K	P0110009	TWP/C1	12/11/1995	01/13/2000
CT25K	P0110009	Vaisala	02/23/2000	04/25/2000
CT25K	P0110009	SGP/B6	08/24/2000	01/05/2001
CT25K	P0110009	TWP/C1	06/24/2001	01/18/2002
CT25K	P0110009	TWP/C2	09/23/2002	04/01/2005
CT25K	P0110009	TWP/C3	12/12/2005	05/18/2006
CT25K	P0110009	Vaisala	07/17/2006	09/15/2006
CT25K	P0110009	TWP/C3	12/20/2006	01/12/2007
CT25K	P0110009	Vaisala	05/04/2007	06/13/2007
CT25K	P0110009	TWP/C3	07/11/2007	08/16/2010

## 4.0 Near-Real-Time Data Plots

Available [data plots and other data products](#).

## 5.0 Data Description and Examples

The figures below show an example of the independent data collection, storage, analysis, and presentation programs available for the Vaisala Ceilometers (CL-View and BL-View). This particular example shows a cloud intensity graph (Figure 1) and a planetary boundary layer analysis graph (Figure 2) of backscattering data collected at the Southern Great Plains site on 04/16/2010 during acceptance testing of the CL31.

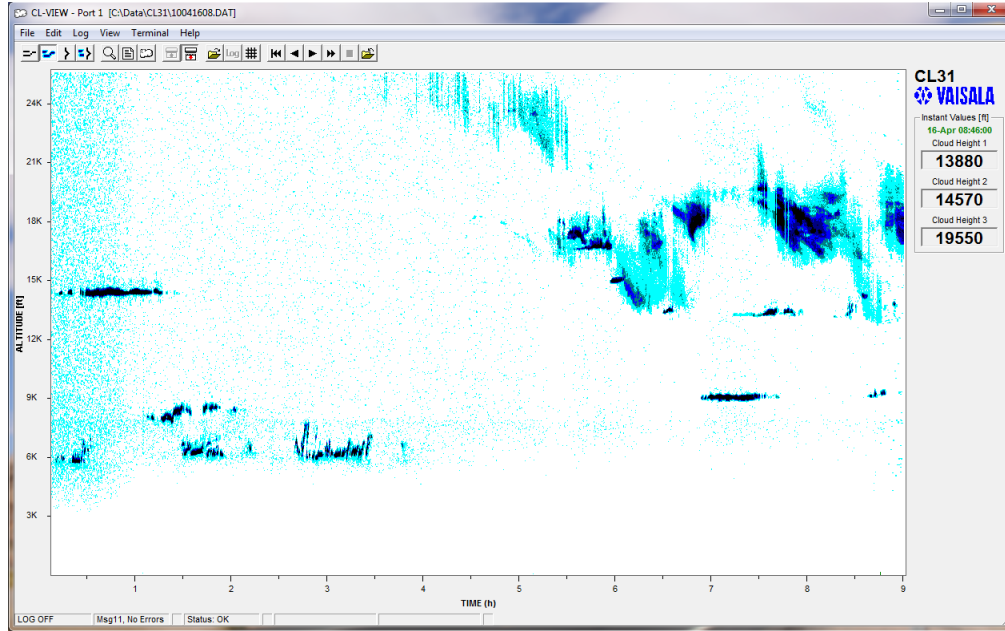


**Figure 1.** CL-View cloud intensity graph (0 – 25500 ft AGL).

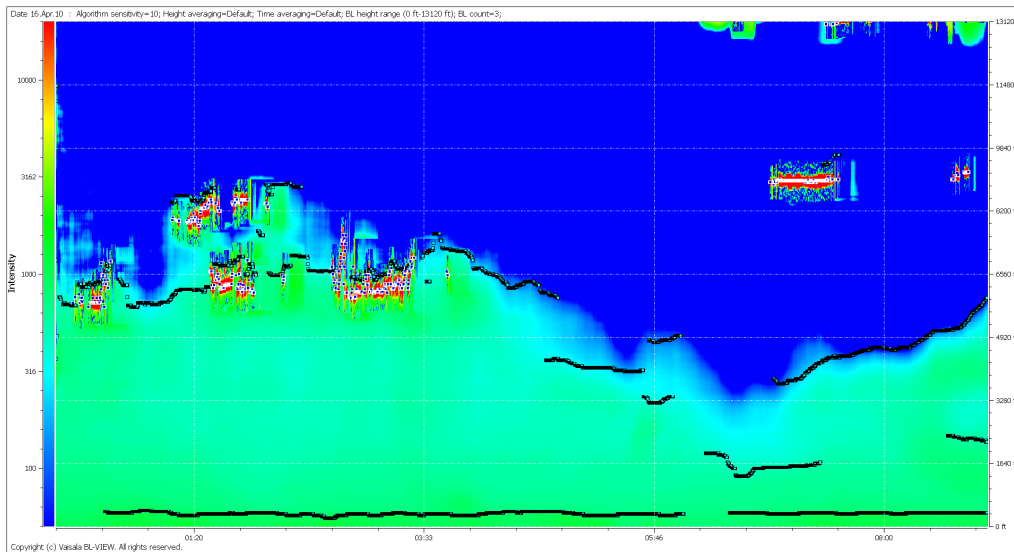


**Figure 2.** BL-View planetary boundary layer analysis graph (0 – 13120 ft AGL).

## 5.1 Data File Contents

The CEIL produces datastream [ceil](#), containing cloud base heights, above ground level (AGL), below 7700 m with 10-m resolution and [ceilpblht](#), containing planetary boundary heights below 4000 m. These datastreams are available from the [ARM Data Archive](#).

### 5.1.1 Primary Variables and Expected Uncertainty

The Vaisala ceilometers measure the backscattered light intensity from a pulsed InGaAs diode laser (910 nanometers [nm]) as a function of distance. These measurements are used to produce derived products that are recorded.

**Table 2.** Primary variables.

Variable Name	Quantity Measured	Unit
backscatter	Backscatter	1/(srad*km*10000)
first_cbh	Lowest cloud base height detected	m
second_cbh	Second-lowest cloud base height	m
third_cbh	Third cloud base height	m
vertical_visibility	Vertical visibility	m
bl_height_1	First boundary layer height candidate	m
bl_height_2	Second boundary layer height candidate	m
bl_height_3	Third boundary layer height candidate	m

#### 5.1.1.1 Definition of Uncertainty

The specified resolution of the measurement of cloud height and vertical visibility is 10 m, so the estimated uncertainty of these measurements is  $\pm 5$  m. The backscatter profile (range and sensitivity normalized) has an estimated uncertainty of  $\pm 0.1 * 10^{-3} \text{srad}^{-1} \text{km}^{-1}$ .

The calibration of the CEIL laser transmitter is checked every year to ensure a range resolution of 10 m (see section 7.3). The instrument-derived product of cloud-ceiling height may drift with time if the relative sensitivity of the instrument degrades considerably. In the worst case, this change would not be observed until differences with the Micropulse Lidar (MPL), which has a range resolution of 75 m, are observed. A comparison was performed between the Vaisala CT25K and CL31 at the SGP site in summer, 2008. This comparison showed a similar shape to cloud features observed by the two systems, with the CL31 indicating a better vertical resolution, yielding better estimates of mixing-layer height. Figure 3 is an example of the comparison of the backscatter of lowest cloud heights from the two instruments on one of the 31 days.

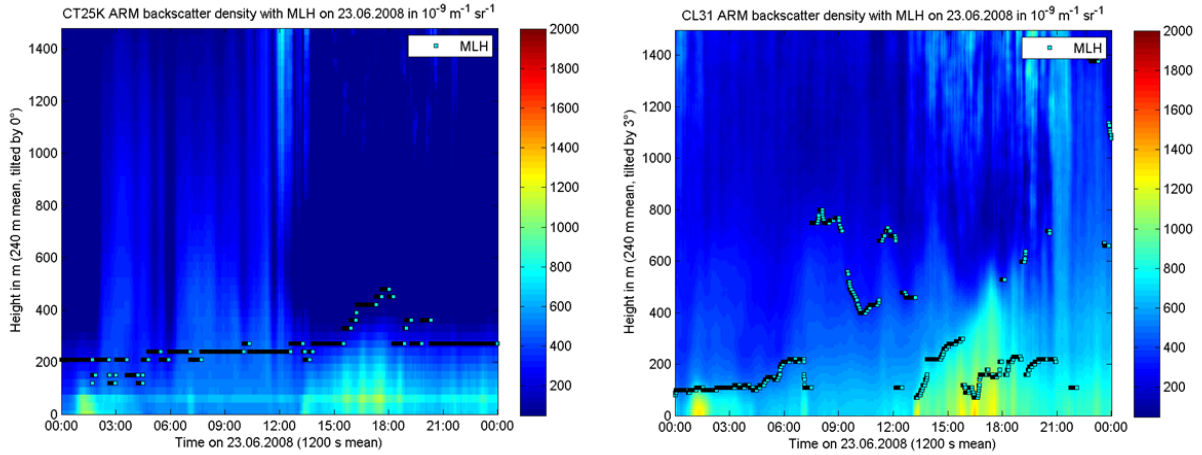


**Figure 3.** Backscatter density in  $10^{-9} \text{ m}^{-1} \text{ sr}^{-1}$  with mixing-layer-height in m from Vaisala CT25K and CL31 Ceilometers on 06/23/2008 at SGP.

### 5.1.2 Secondary/Underlying Variables

**Table 3.** Secondary variables.

Variable Name	Quantity Measured	Unit
time	Time offset from midnight	seconds
range	Distance to the center of the corresponding range bin	m
alt_highest_signal	Altitude of highest signal	m
sum_backscatter	Sum of detected and normalized backscatter	1/srad

### 5.1.3 Diagnostic Variables

**Table 4.** Diagnostic variables.

Variable Name	Quantity Measured	Unit
time_offset	Time offset from base_time	seconds
laser_pulse_energy	Laser pulse energy	%
laser_temperature	Laser temperature	C
window_transmission	Window transmission estimate	%
tilt_angle	Tilt angle	degree
background_light	Background light	mV
status_string	Warning, alarm, and internal status information	unitless
detection_status	Detection status	unitless
status_flag	Ceilometer status indicator	unitless

Variable Name	Quantity Measured	Unit
measurement_parameters	Instrument measurement parameters	unitless
bl_index_1	Quality index for first boundary layer height candidate	unitless
bl_index_2	Quality index for second boundary layer height candidate	unitless
bl_index_3	Quality index for third boundary layer height candidate	unitless

### 5.1.4 Data Quality Flags

Most fields contain a corresponding, sample-by-sample, automated quality check field in the b1 level datastreams. These flags are named **qc\_<fieldname>**. For example, the **first\_cbh** field also has a companion **qc\_first\_cbh** field. Possible values for each sample of the **qc\_<fieldname>** are shown in the table below.

**Table 5.** Data quality flags.

Value	Definition
0	All QC checks passed
1	Sample contained 'missing data' value
2	Sample was less than prescribed minimum value
3	Sample failed both 'missing data' and minimum value checks
4	Sample greater than prescribed maximum value
5	Sample failed both minimum and maximum value checks (highly unlikely)
7	Sample failed minimum, maximum, and missing value checks (highly unlikely)
8	Sample failed delta check (change between this sample and previous sample exceeds a prescribed value)
9	Sample failed delta and missing data checks
10	Sample failed minimum and delta checks
11	Sample failed minimum, delta, and missing value checks
12	Sample failed maximum and delta checks
14	Sample failed minimum, maximum, and delta checks
15	Sample failed minimum, maximum, delta, and missing value checks

The minimum and maximum thresholds are currently defined as follows for datastream **ceil**:

**Table 6.** Data quality thresholds.

Field Name	Units	Min	Max	Delta
first_cbh	m	0	7700	--
second_cbh	m	0	7700	--

Field Name	Units	Min	Max	Delta
third_cbh	m	0	7700	--
vertical_visibility	m	0	7700	--
alt_highest_signal	m	0	7700	--
laser_pulse_energy	%	10	110	100
laser_temperature	C	-10	60	5
tilt_angle	degree	0	4	1
bl_height_1	m	0	4000	-
bl_height_2	m	0	4000	-
bl_height_3	m	0	4000	-

In addition to the above data quality checks, the **qc\_time** field is also supplied. The purpose of this field is to help detect duplicate samples, missing samples, or other sample time problems. The qc\_time field contains a value for each sample time. It has a lower limit of 14 s and an upper limit of 16 s. Refer to the table below for details.

**Table 7.** Time quality flags.

Value	Description
0	Dt is within specified range
1	Dt is 0, duplicate sample
2	Dt is less than specified lower limit
4	Dt is greater than specified upper limit

Additional information is found at the ARM netCDF file header description of the [ceil Data Object Design](#).

### 5.1.5 Dimension Variables

**Table 8.** Dimension variables.

Variable Name	Quantity Measured	Unit
base_time	base time in Epoch	seconds
lat	north latitude	degrees
lon	east longitude	degrees
alt	altitude	meters above Mean Sea Level

## 5.2 User Notes and Known Problems

The status\_flag field is briefly set to “Alarm” during daily preventative maintenance due to water and/or alcohol used to clean the window.

The CEILs at the ARM sites are normally operated in vertical orientation. The tilt angle of the CL31 is measured by a thermal sensor on the transmitter board. A diurnal oscillation of the measured tilt angle from 0 to 3 degrees has been observed that is attributed only to solar heating of the ceilometer, not due to an actual change in the tilt angle. The detected cloud base height is normally automatically compensated for the tilt angle. However, this option was disabled in 2013 to provide for the derivation of the planetary boundary layer height (BCR-1916).

The Vaisala CT25K ceilometers were replaced with model CL31 in 2010 (BCR-1647).

## 5.3 Frequently Asked Questions

**What is the difference between cloud height determination algorithms using the ceilometer and the Micropulse Lidar (MPL)?**

The MPL uses a threshold variation to identify the cloud bottom, and the ceilometers use a calculated vertical visibility threshold of 100 m. This means that the ceilometer will not classify thin cloud regions that the MPL would identify and usually give a slightly higher cloud bottom height.

**Can direct sun damage the optics and detection systems of a ceilometer?**

No. Optical filters provide solar protection of the transmitter and receiver diodes of the CL31, so there is no need for additional protection of the window. However, direct solar radiation exposure may cause alarms and temporarily invalidate the data.

**Are the ceilometers eye-safe?**

Yes. However, the outgoing beam must never be viewed through magnifying optics such as binoculars or a camera.

**Can the ceilometer returns be used to detect aerosol mixed-layer depths in the absence of clouds?**

Yes, to some extent. At the ARM sites, the CL31 measurement algorithms have been optimized for performance in aerosol and mixing-layer applications.

**How does the CEIL compare with other ceilometers during low cloud conditions such as are often observed in the Arctic?**

The CEIL uses overlapping transmitting and receiving optics so that beam overlap occurs at shorter distances, thereby improving detection of thin clouds at only about 10 m above the ceilometer.

**Are the cloud heights provided by the CEIL measured above sea level or above ground level?**

The cloud height values are measured above the optics assembly and are not adjusted for altitude.

### **Are the cloud heights corrected for the tilt angle of the CEIL?**

No, the cloud heights are not currently corrected for tilt angle. In 2010, when the Vaisala CT25Ks were replaced with model CL31, we realized that the tilt angle measurement was not accurate and displayed a diurnal pattern that did not represent the instrument's vertical orientation. The CT25K tilt angle measurement is an accurate representative of the angle from vertical, so the cloud heights are automatically corrected. But for the CL31, the automatic correction option was disabled during the initial configuration at each site (BCR-1647) and was required for the determination of the planetary boundary layer heights (BCR-1916).

### **What is the ceilometer's field-of-view?**

The vertically pointed laser transmission has a beam divergence of  $\pm 4$  milliradian (mrad)  $\times$   $\pm 7$  mrad and a receiver field-of-view divergence of  $\pm 0.83$  mrad. The optical system has a focal length of 300 mm and effective lens diameter of 96 mm.

## **6.0 Data Quality**

### **6.1 Data Quality Health and Status**

The following links go to current data quality health and status results.

- [DQ Explorer](#)
- [NCVweb](#) for interactive data plotting using.

The tables and graphs shown contain the techniques used by ARM's data quality analysts, instrument mentors, and site scientists to monitor and diagnose data quality.

### **6.2 Data Reviews by Instrument Mentor**

On a weekly basis, the instrument mentor inspects plots of the data from the CEILs at the SGP, North Slope of Alaska (NSA), Eastern North Atlantic (ENA), and ARM Mobile Facility (AMF) sites. Time series plots are inspected to compare backscatter density and cloud heights measured by the CEIL and MPL.

The MPL uses photon counting, rather than photocurrent detection, and defines a cloud by identifying a sudden increase in backscatter, rather than cloud droplet scattering that reduces visibility to less than 100 m. The increased sensitivity and looser definition of a cloud causes the MPL to often report clouds that are not reported by the CEIL. However, both instruments should normally report clouds and cloud bases that correspond closely.

The data are also examined for internal consistency, specifically whether clouds are observed at heights up to the limit of the system (7.7 km), the backscatter plots show expected variability, data gaps are minimal, and warning flags for window contamination are minimal.

Data Quality Problem Reports (DQPRs) and Data Quality Reports (DQRs) are submitted when needed.

### 6.3 Data Assessments by Site Scientist / Data Quality Office

All DQ Office and most Site Scientist techniques for checking have been incorporated within [DQ Explorer](#) and can be viewed there.

### 6.4 Value-Added Procedures and Quality Measurement Experiments

Many of the scientific needs of the ARM Climate Research Facility are met through the analysis and processing of existing data products into "value-added" products, or VAPs. Despite extensive instrumentation deployed at the ARM sites, there will always be quantities of interest that are either impractical or impossible to measure directly or routinely. Physical models using ARM instrument data as inputs are implemented as VAPs and can help fill some of the unmet measurement needs of the facility. Conversely, ARM produces some VAPs not to fill unmet measurement needs, but to improve the quality of existing measurements. In addition, when more than one measurement is available, ARM also produces "best estimate" VAPs. A special class of VAP called a Quality Measurement Experiment (QME) does not output geophysical parameters of scientific interest. Rather, a QME adds value to the input datastreams by providing for continuous assessment of the quality of the input data based on internal consistency checks, comparisons between independent similar measurements, or comparisons between measurement with modeled results, and so forth. For more information see [VAPs and QMEs](#).

The most useful quality measurement experiment for the ceilometer is comparison of cloud heights detected with an MPL and the CEIL. However, it must be kept in mind that the MPL can detect backscatter from thin clouds that are not discernible from the processed CEIL backscatter. One reason for this is the fact that the CEIL is designed to detect clouds that obscure pilot visibilities to less than 100 m and is just not as sensitive as the MPL (photon counting versus photo current detection, respectively). Also, there is a change in daytime/nighttime sensitivity in the data. When there are both MPL and CEIL data, the most sensitivity to thin clouds will always come from the MPL. The combination of the MPL and the CEIL is still valuable not only in maintaining a continuous datastream, but also the higher resolution of the CEIL is useful for lower-level cloud detection and possibly cloud-free mixing-depth estimates under some circumstances.

Another quality measurement experiment can be performed by comparing the CEIL cloud base height and the calculated lifting condensation level from surface humidity and temperature measurements. The lifting condensation level temperature can be calculated as  $T_l = 1 / [(1/(T_k - 55)) - \ln(U/100)/2840]$  where  $T_k$  is the absolute surface temperature (K) and  $U$  is the surface relative humidity (%). The height associated with the lifting condensation level can be calculated from an adiabatic lapse rate assumption.

## 7.0 Instrument Details

### 7.1 Detailed Description

#### 7.1.1 List of Components

The system components consist primarily of the Measurement Unit and Shield, which include the following replaceable parts:

**Table 9.** Vaisala CL31 main parts.

<b>Component</b>	<b>Part Code</b>
Receiver	CLR321
Transmitter	CLT321
Optics Unit	CLO321
Engine Board	CLE321
Laser Monitor Board	CLM311
Window Assembly	CLW311
Window Blower	CLB311
Internal Heater	CLH311
AC Power	CLP311
Battery	226116
Power Cable	CT35324
Data Cable	CT3838
Termination Box	TERMBOX-1200

Presently, the spare parts supply includes one each transmitter, receiver, and heater. The optional parts supply includes a maintenance cable, QMZ101, and an optical termination hood, CLTERMHOOD, for diagnostics and calibration.

#### 7.1.2 System Configuration and Measurement Methods

The CEIL measures cloud-bottom heights and vertical visibilities (above ground level). These instruments employ pulsed diode laser lidar (light detection and ranging) technology, where short, powerful laser pulses are sent out in a vertical or slanted direction. The directly backscattered light caused by haze, fog, mist, virga, precipitation, and clouds is measured as the laser pulses traverse the sky. This is an elastic backscatter system, and the return signal is measured at the same wavelength as the transmitted beam. The ceilometer backscatter profile (i.e., signal strength versus height) is stored, and the cloud bases are detected. Knowing the speed of light, the time delay between the launch of the laser pulse and the detection of the backscatter signal gives the cloud-base height (see Theory of Operation, Section 7.2).

The CEIL is able to detect three cloud layers simultaneously. Besides cloud layers, it can detect whether there is precipitation or other obstructions to vision. The embedded software includes several service and maintenance functions and gives continuous status information from internal monitoring.

To optimize performance for measuring aerosol and boundary-layer structure, the CL31 ceilometers have been configured with the following user command assignments:

**Table 10.** Vaisala CL31 configuration settings.

<b>Command</b>	<b>Parameter</b>	<b>Description</b>
set unit_id	<character assigned to unit SN>	set unit ID
set message type	msg1_10x770	set message format to type 1 with 10m x 7700m profile
set message interval	16	set message delivery interval to 16 s
set message port	data	set message delivery into data port
set message units	meters	set reported heights unit to m
set message angle_corr	off	set heights correction for tilt angle to off
set message profile noise_h2	on	set range gate normalization to on
set factory algo_sensit general	1	set algorithm parameter to 1
set factory algo_sensit second_layer	4	set algorithm parameter to 4
set factory algo_sensit cloud	3	set algorithm parameter to 3
set factory algo_sensit high_cloud	5	set algorithm parameter to 5
set option humitter	on	set humitter option to on

The instruments are placed on a foundation. The foundation should be a concrete pad at least 200 mm thick (the hole depth for the mounting bolts is 160 mm). The width should be 500 mm or larger (the whole spacing is a square pattern 283 mm on a side). The pad is usually oriented so that one side of the pad points north-south. The ceilometer is delivered with the measurement unit attached to the shield. It is recommended that the measurement unit is first removed, the shield mounted onto the foundation so that the door faces north in the northern hemisphere and south in the southern hemisphere, and then the measurement unit installed into the shield.

### 7.1.3 Specifications

**Table 11.** Specifications of CL31 ceilometer, as operated at ARM sites.

Property	Value
Range	0–7.5 km
Vertical resolution	10 m
Accuracy (against reflector)	±1% or ±5m
Measurement interval	2 s
Reporting interval	16 s
Wavelength	910 nm at 25°C
Transmitter	Indium Gallium Arsenide pulsed diode laser
Receiver	Silicon Avalanche Photodiode
Field of view divergence	±0.83 mrad
Dimensions	1190 x 335 x 324 mm
Weight	32 kg
Power	115 VAC, 310 W max.

## 7.2 Theory of Operation

### Basic Principle of Operation

The operating principle of the ceilometer is based on measurement of the time needed for a short pulse of light to traverse the atmosphere from the transmitter of the ceilometer to a backscattering cloud base and back to the receiver of the ceilometer. The general expression connecting time delay ( $t$ ) and backscattering height ( $h$ ) is  $h = ct/2$ , where  $c$  is the speed of light. With  $c = 2.9929 \times 10^8$  m/s, a reflection from 7620 m will be seen by the receiver after  $t = 50.9 \mu\text{s}$ .

### Practical Measurement Signal

Generally, particles at all heights backscatter light, and so the actual return signal may look like that shown in the figure below.

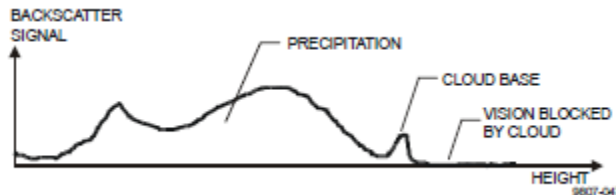


**Figure 4.** Typical measurement signal.

The instantaneous magnitude of the return signal will provide information on the backscatter properties of the atmosphere at a certain height. From the return signal, information about fog and precipitation, as well

as cloud, can be derived. Since fog and precipitation attenuate the light pulse, the cloud base signal will appear lower in magnitude in the return echo. However, the fog and precipitation information also provides data for estimating this attenuation and computing the necessary compensation, up to a limit. In its normal full-range operation, the ceilometer digitally samples the return signal every 67 nanoseconds (ns) from 0 to 50  $\mu$ s, providing a spatial resolution of 10 m from ground to 7700 m distance. This resolution is adequate for measuring the atmosphere, since visibility in the densest clouds is of the same order.

### **Noise Cancellation**

For safety and economic reasons, the laser power used is so low that the noise of the ambient light exceeds the backscattered signal. To overcome this, a large number of laser pulses are used, and the return signals are summed. The desired signal will be multiplied by the number of pulses, whereas the noise, being random, will partially cancel itself. The degree of cancellation for white (Gaussian) noise equals the square root of the number of samples; thus, the resulting signal-to-noise ratio improvement will be equal to the square root of the number of samples. However, this processing gain cannot be extended endlessly since the environment changes, and, for example, clouds move.

### **Height Normalization**

Assuming a clear atmosphere, it can be seen that the power is inversely proportional to the square of the distance or height (i.e., the strength of a signal from 10,000 feet is generally one hundredth of that from 1,000 feet). The height square dependence is eliminated by multiplying the value measured with the square of the height (height normalization). However, noise, being height independent from a measurement point of view, will then be correspondingly accentuated with increasing height.

### **The Backscatter Coefficient**

The volume backscatter coefficient,  $\beta(z)$ , represents the portion of light that is reflected back towards the ceilometer from a distance  $z$  (e.g., by water droplets). It is obvious that the denser a cloud is, the stronger the reflection will be. The relationship can be expressed as:  $\beta(z) = k \cdot \sigma(z)$

where

$k$  = "constant" of proportionality and

$\sigma$  = is the extinction coefficient (i.e., the attenuation factor in a forward direction).

The extinction coefficient relates to visibility in a straightforward manner. If visibility is defined according to a 5% contrast threshold (World Meteorological Organization definition for Meteorological Optical Range [MOR]), equals daylight horizontal visibility), then  $\sigma = 3 / V$

where

$V$  = MOR visibility (5% contrast)

The "constant" of proportionality,  $k$ , also called the Lidar Ratio, has been subjected to a lot of research. Although the Lidar Equation can be solved without knowing its value, it must remain constant with height if accurate estimates of the extinction (or visibility) profile are to be made.

It has been found that in many cases,  $k$  can be assumed to equal 0.03, tending to be lower in high humidities, to 0.02; and higher in low humidities, to 0.05. However, in precipitation of various kinds,  $k$  will have a wider range of values. Assuming a value 0.03 ( $\text{srad}^{-1}$ ) for  $k$  and visibility in clouds being in the range 15–150 m, gives the range of value for  $\beta$ :

$$\beta = 0.0006 - 0.006 \text{ m}^{-1}\text{srad}^{-1} = 0.6 - 6 \text{ km}^{-1}\text{srad}^{-1}$$

### **Extinction Normalization and Vertical Visibility**

Any fog, precipitation, or similar obstruction to vision between ground and cloud base may attenuate the cloud base signal and produce backscatter peaks that far exceed that from the cloud. Virtually any backscatter height profile is possible, up to some physical limits. To distinguish a significant cloud return signal, the attenuation of fog, precipitation, etc., has to be taken into account by normalizing with regard to extinction. The profile thus obtained is proportional to the extinction coefficient at various heights and enables the use of fairly straightforward threshold criteria to determine what is cloud and what is not.

By assuming a linear relationship between backscatter and extinction coefficient according to the previous formula and that the ratio,  $k$ , is constant over the range observed, it is possible to obtain an extinction coefficient profile through a mathematical computation. This is also called inverting the backscatter profile to obtain the extinction coefficient profile and answers the question: "What kind of extinction coefficient profile would produce the backscatter profile measured?"

No assumption as to the absolute value of the ratio,  $k$ , needs to be made if  $k$  is constant with height. The assumptions that have to be made are fairly truthful, and in any case, accurate enough for the purpose of cloud detection. Likewise, the inversion is also independent of several instrumental uncertainties including transmitted power and receiver sensitivity.

An estimate of vertical visibility can easily be calculated from the extinction coefficient profile because of the straightforward extinction-coefficient-to-visibility relationship, provided that a constant contrast threshold is assumed. Visibility will simply be that height where the integral of the extinction coefficient profile, starting from ground, equals the natural logarithm of the contrast threshold, sign disregarded.

Tests and research have, however, shown that the 5% contrast threshold widely used for horizontal measurement is unsuitable for vertical measurement if values close to those estimated by a ground-based observer are to be obtained. The ceilometer uses a contrast threshold value that, through many tests, has been found to give vertical visibility values closest to those reported by ground-based human observers. A wide safety margin is obtained with regard to pilots looking down in the same conditions since the contrast objects, especially runway lights, are much more distinct on the ground.

## **7.3 Calibration**

### **7.3.1 Theory**

The calibration can be verified by tilting the ceilometer at a hard target at a known distance. Comparison with MPL heights during low cloud situations can also be informative. The hard target test is performed by removing the measurement unit from the shield, placing the unit horizontally, turning off tilt angle

correction, and detecting the return from a solid object of known distance at least 300 m from the ceilometer.

### 7.3.2 Procedures

See Vaisala “CL31 verification of proper operation”.

### 7.3.3 History

**Table 12.** Calibration of CL31 laser transmitter.

CL31 Serial number	CLT321 Serial number	CLT321 Calibration Factor	Date
F1040001	F0550002	2074	03/08/2010
F1040002	F0550007	2058	03/08/2010
F1040003	F0550006	2208	03/09/2010
F1040004	F0550005	1925	03/09/2010
F1040005	E4140020	2070	03/09/2010
F1040006	F0310026	2045	03/09/2010
H2310002	H1030004	1902	06/07/2012
H2320001	H1030003	2070	06/08/2012
J3110011	J2140022	1987	08/01/2013
-	E4310003	2095	03/09/2010

## 7.4 Operation and Maintenance

### 7.4.1 User Manual

See [Vaisala CL31 Ceilometer documentation](#).

### 7.4.2 Routine and Corrective Maintenance Documentation

See [Corrective Maintenance Reporting sites](#).

### 7.4.3 Software Documentation

See Vaisala [CL-View](#) and [BL-View](#) documentation.

## 7.5 Glossary

See the [ARM Glossary](#).

## 7.6 Acronyms

See the [ARM Acronyms](#).

## 7.7 Citable References

Bowen, R., R Calhoun, and J Rasanen. 2002. "Ceilometer boundary layer measurements during the DOE/VTMX/URBAN Field Experiment in Salt Lake City." In *Fourth Symposium on Urban Environment*, American Meteorological Society.

Emeis, S, C Munkel, S Vogt, WJ Muller, and K Schafer. 2004. "Atmospheric boundary-layer structure from simultaneous SODAR, RASS, and ceilometer measurements." *Atmospheric Environment* 38(2): 273-286, [doi:10.1016/j.atmosenv.2003.09.054](https://doi.org/10.1016/j.atmosenv.2003.09.054).

Emeis, S, K Schäfer, and C Munkel. 2009. "Observation of the structure of the urban boundary layer with different ceilometers and validation by RASS data." *Meteorologische Zeitschrift* 18(2): 149-154, [doi:10.1127/0941-2948/2009/0365](https://doi.org/10.1127/0941-2948/2009/0365).

Munkel, C. 2007. "Mixing height determination with lidar ceilometers – results from Helsinki Testbed." *Meteorologische Zeitschrift* 16(4): 451-459, [doi:10.1127/0941-2948/2007/0221](https://doi.org/10.1127/0941-2948/2007/0221).

Munkel, C, N Eresmaa, J Rasanen, and A Karppinen. 2007. "Retrieval of mixing height and dust concentration with lidar ceilometer." *Boundary-Layer Meteorology*: [doi:10.1007/s10546-006-9103-3](https://doi.org/10.1007/s10546-006-9103-3).

Van Tricht, K, IV Gorodetskaya, S Lhermitte, DD Turner, JH Schween, and NPM van Lipzig. 2014. "An improved algorithm for polar cloud-base detection by ceilometer over the ice sheets." *Atmospheric Measurement Techniques* 7: 1153-1167, [doi:10.5194/amt-7-1153-2014](https://doi.org/10.5194/amt-7-1153-2014).



U.S. DEPARTMENT OF  
**ENERGY**

---

Office of Science